

Intergenic accumulation of RNAPII maintains the potential for swift transcriptional re-start upon release from quiescence

Baquero Pérez, Manuela ¹, Laenen, Gertjan ¹ **, Loïodice, Isabelle ¹ **, Mickaël Garnier ¹, Szachnowski, Ugo ², Morillon, Antonin ², Ruault, Myriam ¹, Taddei, Angela ¹

Affiliations

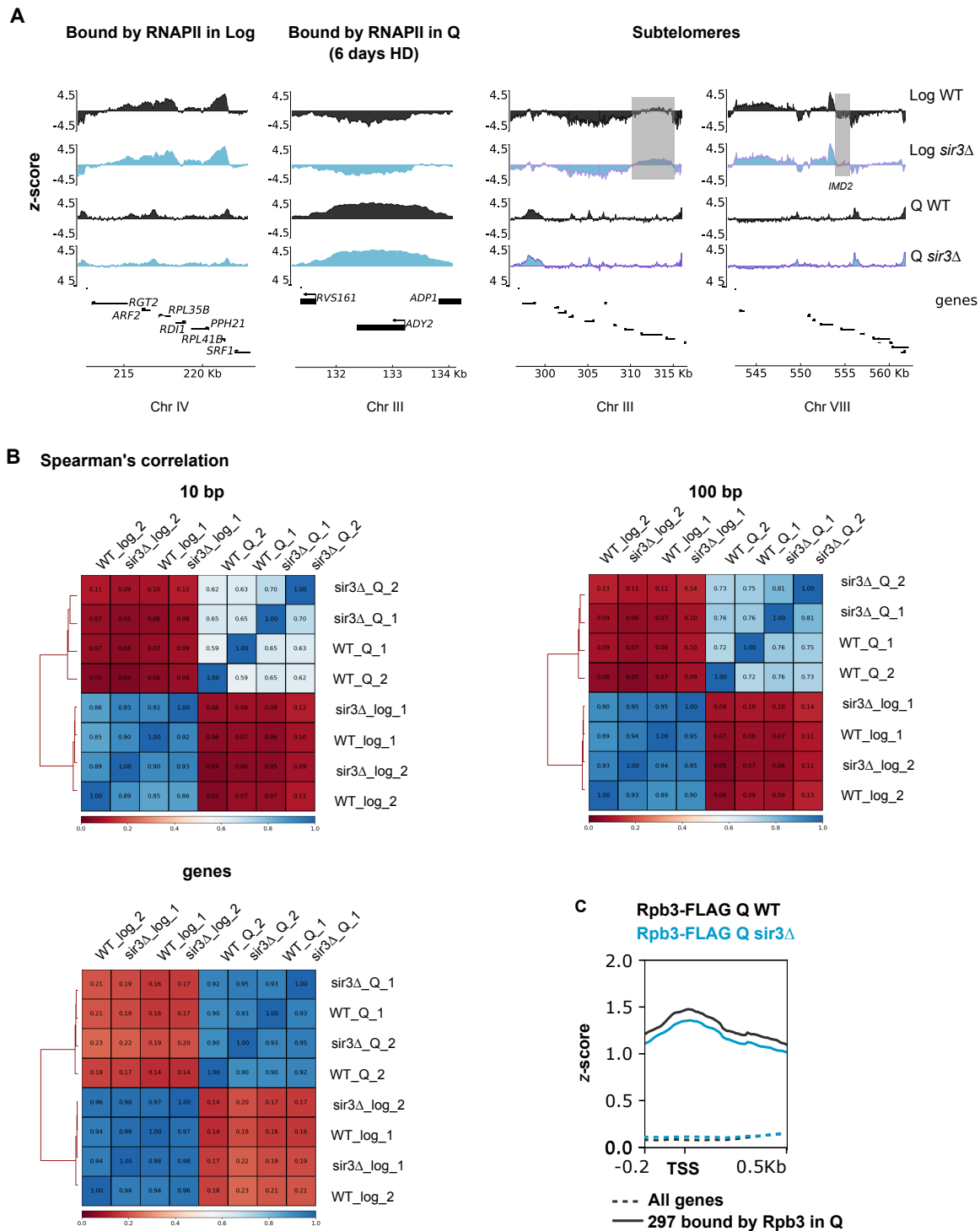
¹ Institut Curie, Université PSL, Sorbonne University, CNRS, UMR3664 Nuclear Dynamics, Paris, France

² Institut Curie, Université PSL, Sorbonne University, CNRS, UMR3244 DIG-Cancer, Paris, France

Supplemental Material

Supplemental Figure S1	2
Supplemental Figure S2	3
Supplemental Figure S3	5
Supplemental Figure S4	13
Supplemental Figure S5	16
Supplemental Figure S6	18
Supplemental Materials and Methods	21
HD gradient enrichment.....	21
Imaging and Rap1-GFP foci quantification.....	21
Sample harvesting for chromatin immunoprecipitation.....	22
ChIP-seq	23
ChIP-qPCR experiments	24
ChIP-seq data processing	25
scRNA-seq experiments.....	30
scRNA-seq data processing	30
RNA-seq data processing	32

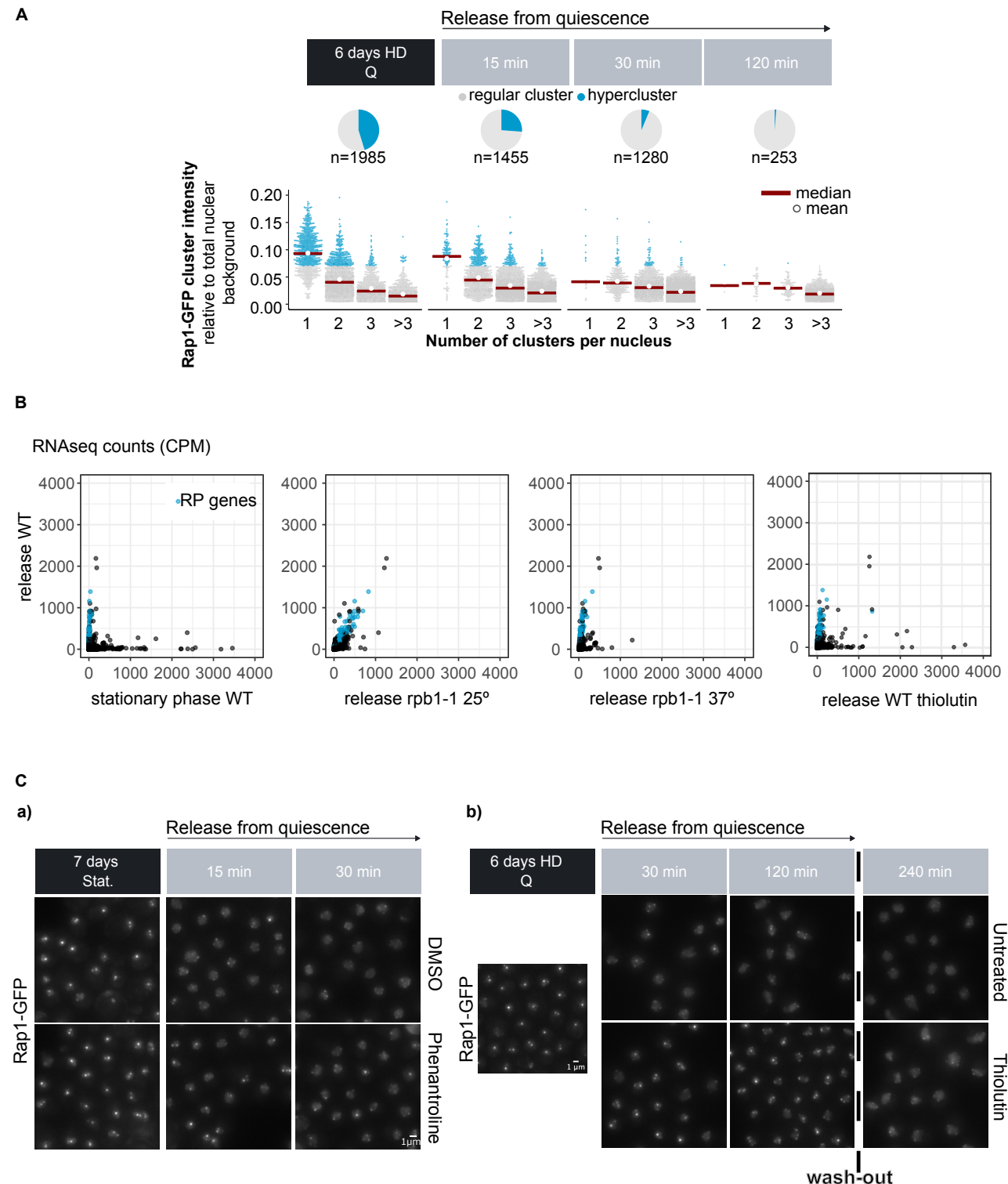
Supplemental Figure S1



B. Clustered heatmap of Spearman's correlations between WT and *sir3Δ* replicates over 10 bp, 100 bp bins or over coding genes. Two biological replicates are shown.

C. Average RNAPII (Rpb3-FLAG) binding aligned over TSS -200, +500 Kb for 297 genes bound by Rpb3-FLAG in Q (thresholded at 50 average counts per gene).

Supplemental Figure S2



Supplemental Figure S2

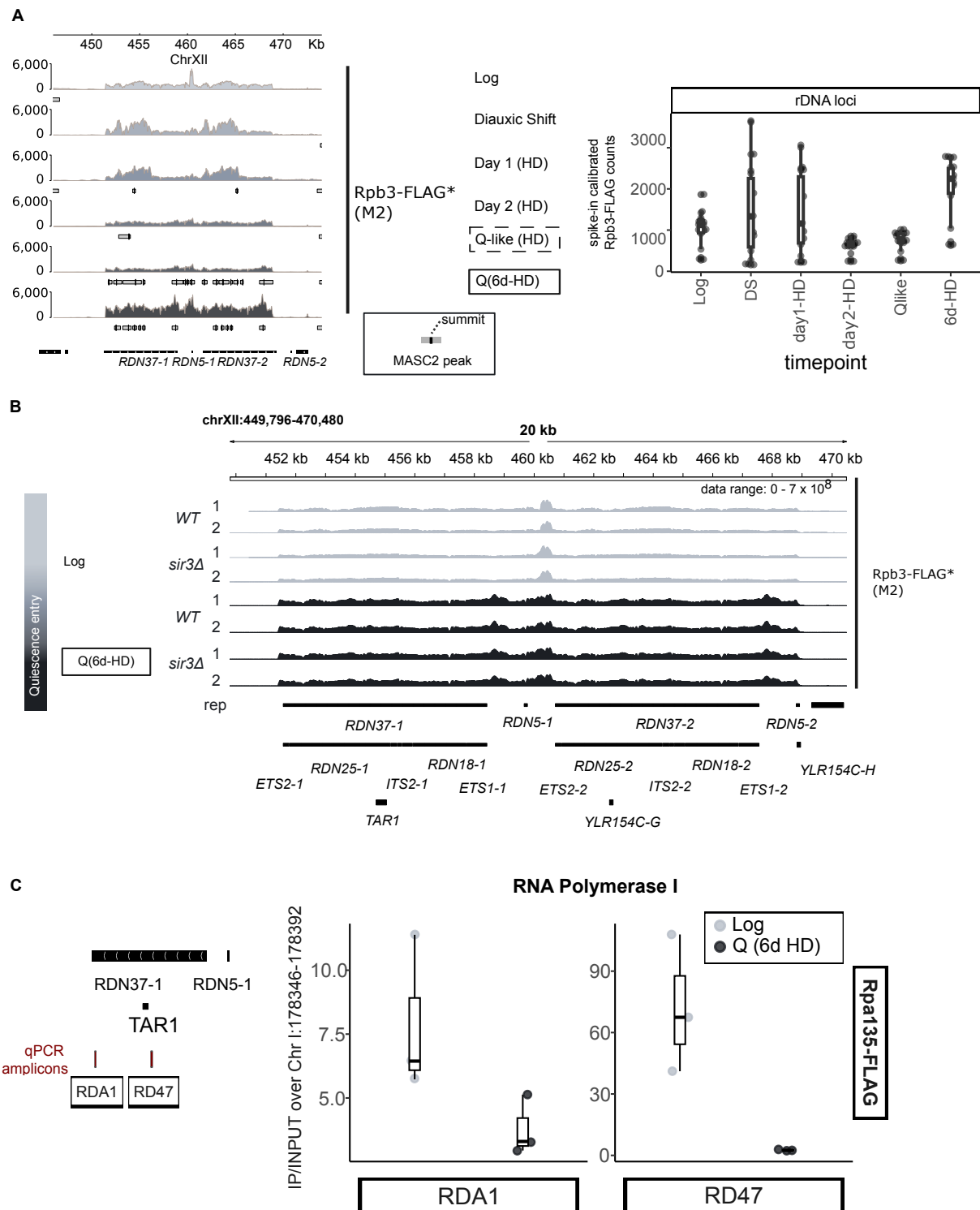
A. Cluster intensities relative to total nuclear signal classified according to the number of clusters found per nucleus. Hyperclusters, in blue, are defined as in fig. 1A (see methods). Quantifications correspond to N=3 biological replicates.

B. CPM normalized RNAseq counts over protein coding genes in transcription inhibition experiments. Blue points correspond to Ribosomal Protein genes (RP).

C. a) Telomere hypercluster dismantling in rich medium (YPD) in cells inhibited (Phenanthroline) or not (DMSO control) for transcription. Representative Rap1-GFP images after 15 or 30 min of refeeding of stationary phase cells. Brightness for all Rap1-GFP images is set at 1600 maximum.

b) Telomere hypercluster dismantling in rich medium (YPD) in cells inhibited (Thiolutin) or not (Untreated) for transcription. Representative Rap1-GFP images after 30, 120 min of refeeding of quiescent (6d-HD) cells and 2h after removal of the inhibitor (240 min). Brightness for all Rap1-GFP images is set at 1600 maximum.

Supplemental Figure S3



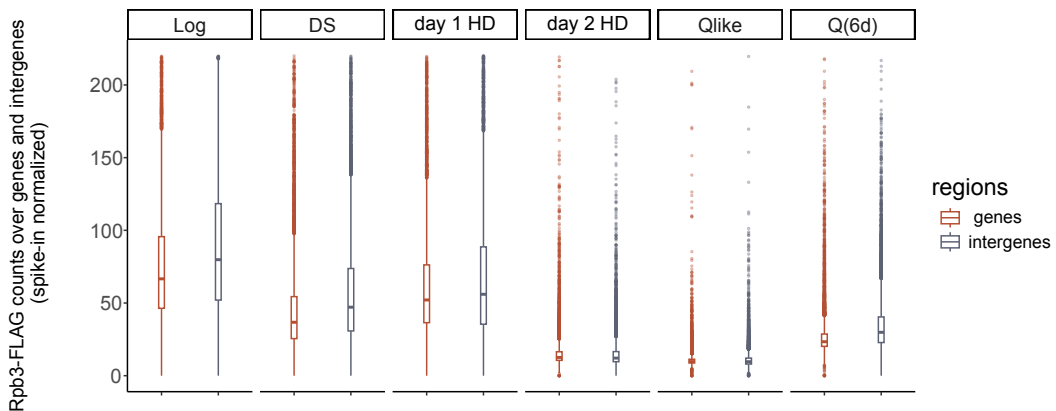
Supplemental Figure S3

A. (left) Genome browser view of spike-in calibrated Rpb3-FLAG over *RDN1* locus. *This study. Gray boxes below every coverage line show called peaks over untagged samples control (MACS2, methods). **(right)** Spike-in calibrated Rpb3-FLAG counts normalized to gene size over all annotations in the *RDN1* locus. Horizontal line in boxplots shows median of each distribution.

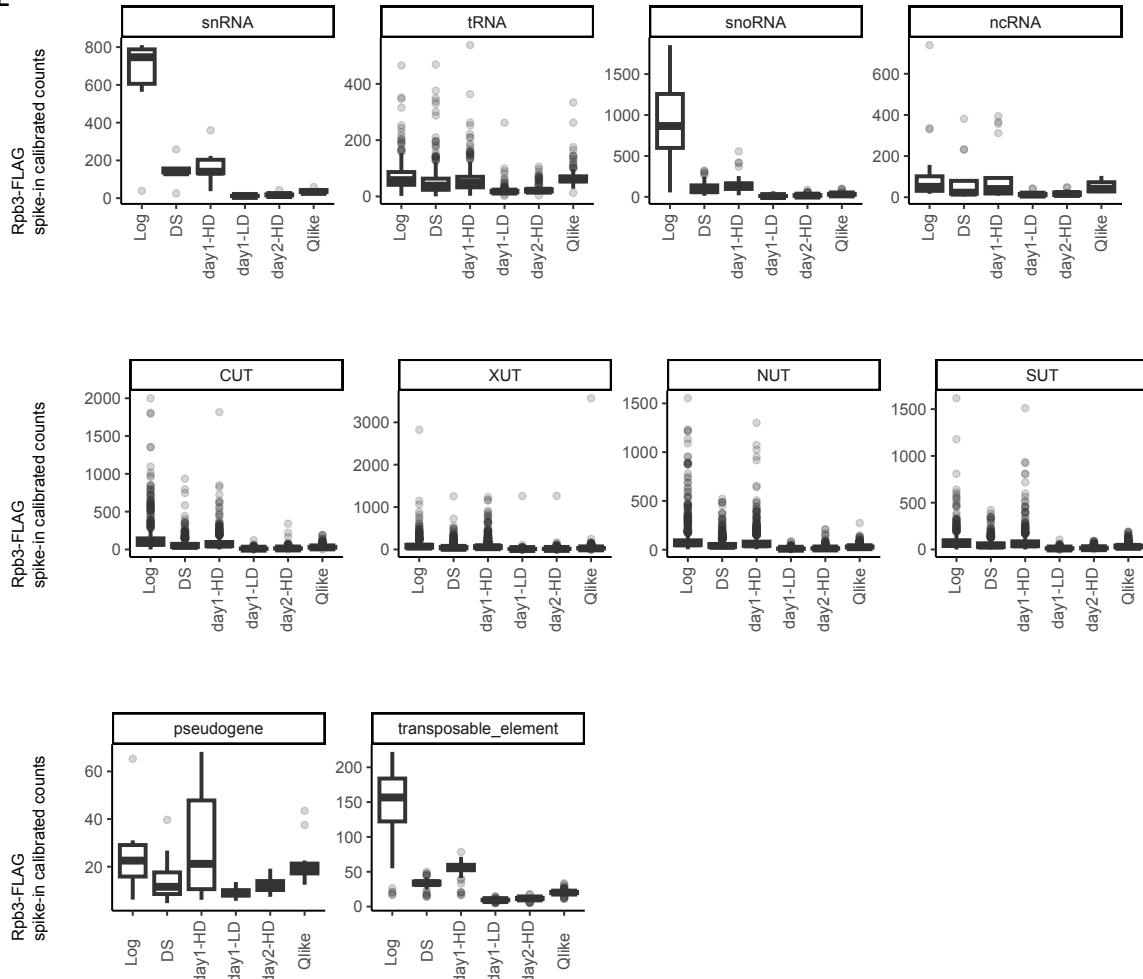
B. Genome browser view of spike-in calibrated Rpb3-FLAG in WT and *sir3* Δ samples over *RDN1* locus.
 *This study. Two biological replicates are shown.

C. ChIP-qPCR IP/INPUT signal of RNA Polymerase I (Rpa135-FLAG) normalized to an intergenic region in chr01 (methods).

D



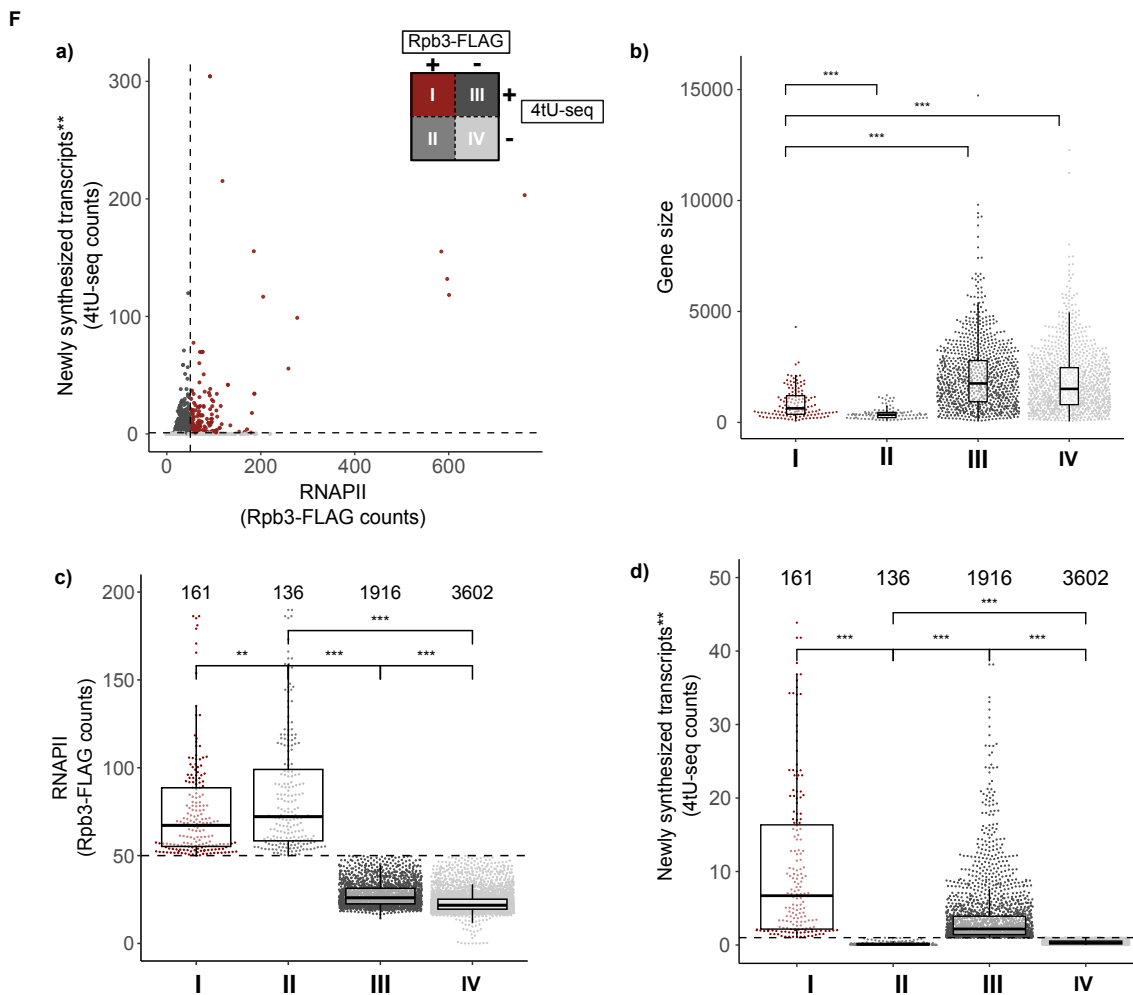
E



Supplemental Figure S3

D. Rpb3-FLAG spike-in calibrated counts normalized to region size (genes, red, or intergenes, blue). Two biological replicates are shown

E. Spike-in calibrated Rpb3-FLAG counts normalized to gene size over all non-coding annotations. Horizontal line in boxplots shows median of each distribution.



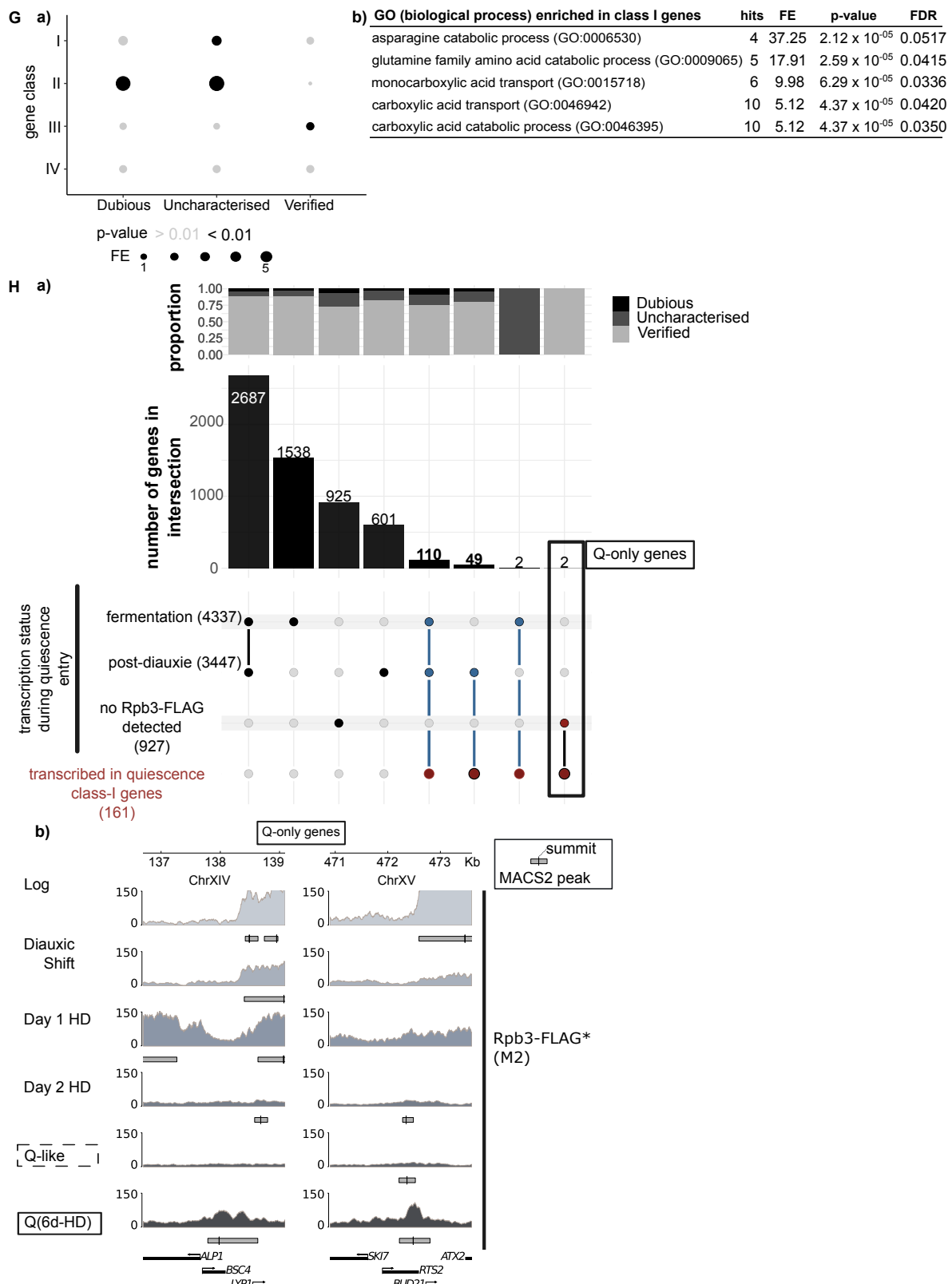
Supplemental Figure S3

F. a) Thresholding of counts for recently synthesized transcripts (4tU-seq) and RNAPII binding (Rpb3-FLAG) normalized to gene size. Dashed lines correspond to the thresholds used for binarizing data.

b) Gene size for the categories identified in Fig 3A. and shown in a) *** p-value $<1.10^{-6}$, Wilcox test

c) Rpb3-FLAG counts for the categories identified in a) Dashed lines correspond to the thresholds used for binarizing data. *** p-value $<1.10^{-6}$, wilcox test

d) 4tU-seq counts for the categories identified in a) Dashed lines correspond to the thresholds used for binarizing data. *** p-value $<1.10^{-6}$, wilcox test.



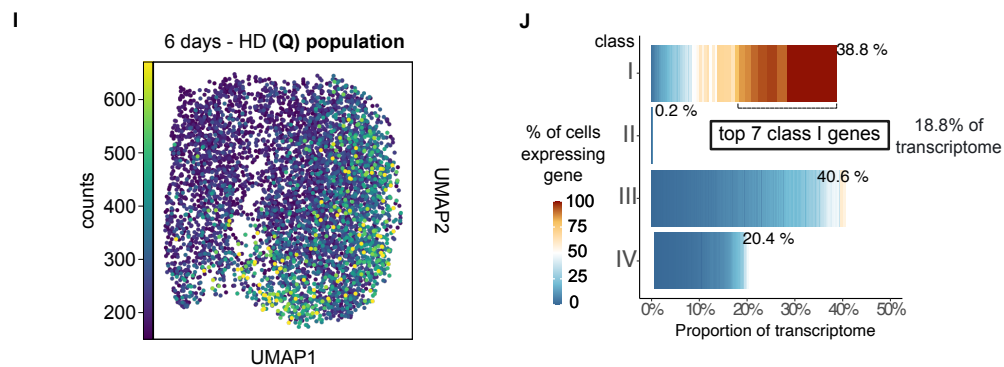
Supplemental Figure S3

G. a) ORF type enrichment per category described in A. Size of dots is proportional to fold enrichment (FE) in each class. P-value given for hypergeometric test

b) Top 5 Gene Ontology terms enriched in class I genes.

H. a) UpSet plot shows overlap of class-I genes with genes transcribed during fermentation (Log) or respiration (post-diauxie, day 1 HD), based on the average Rpb3-FLAG counts as in A. For each intersection, the ORF type enrichment is shown.

b) Snapshots of Q-only genes, *BSC4* and *RTS2*, showing mappings of Rpb3-FLAG for all timepoints in the kinetics of quiescence entry (*This study). Gray boxes below every coverage line show called peaks over untagged samples control (MACS2, methods).



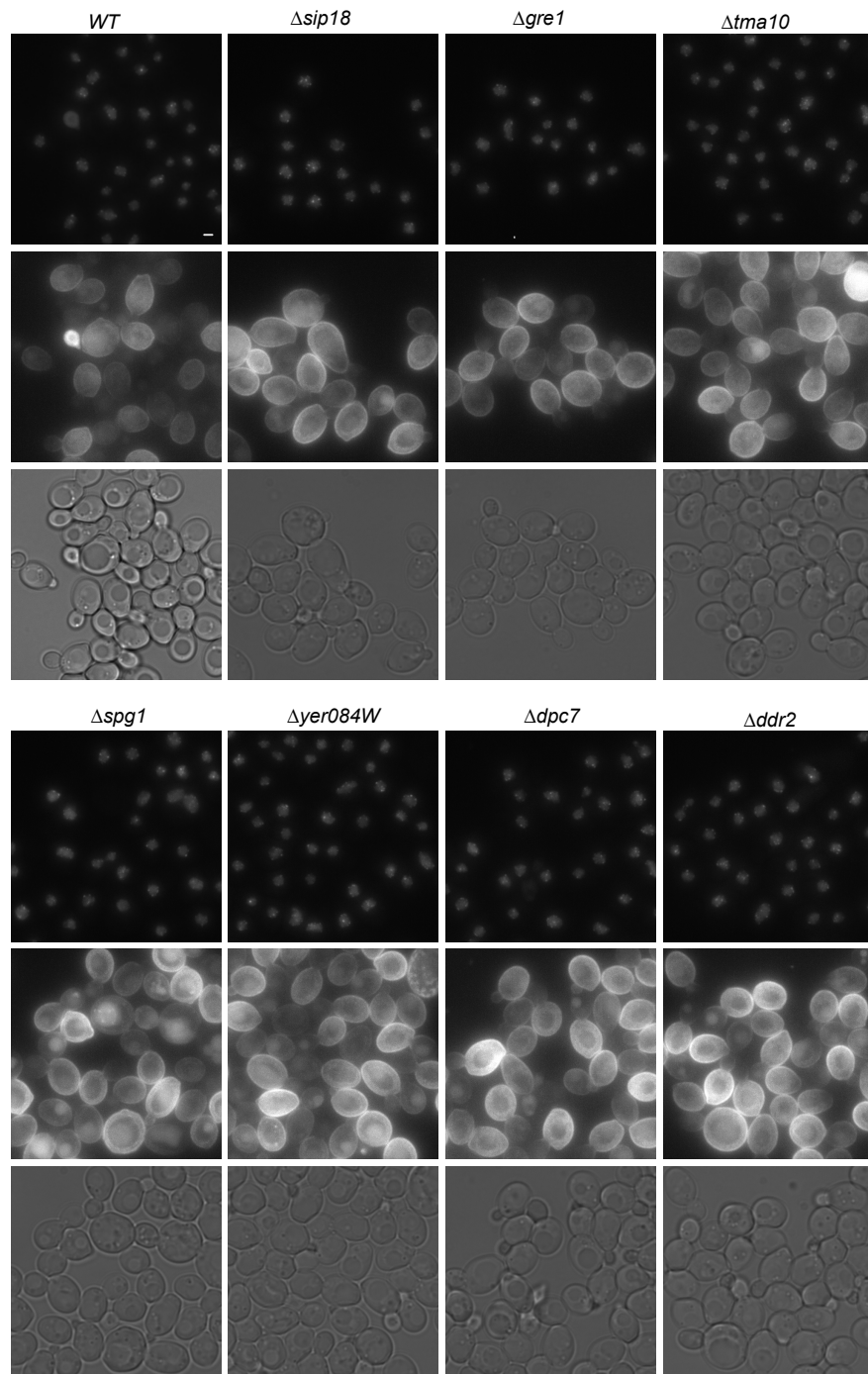
Supplemental Figure S3

I. UMAP representation of cells in the quiescent population assessed by scRNA-seq. Colour scale represents the counts per cell.

J. Proportion of the transcriptome of the average cell in the quiescent population held by each class defined in A. The size of each stacked bar is proportional to the proportion of the transcriptome held by the gene. Colour scale represents the percentage of cells expressing the gene.

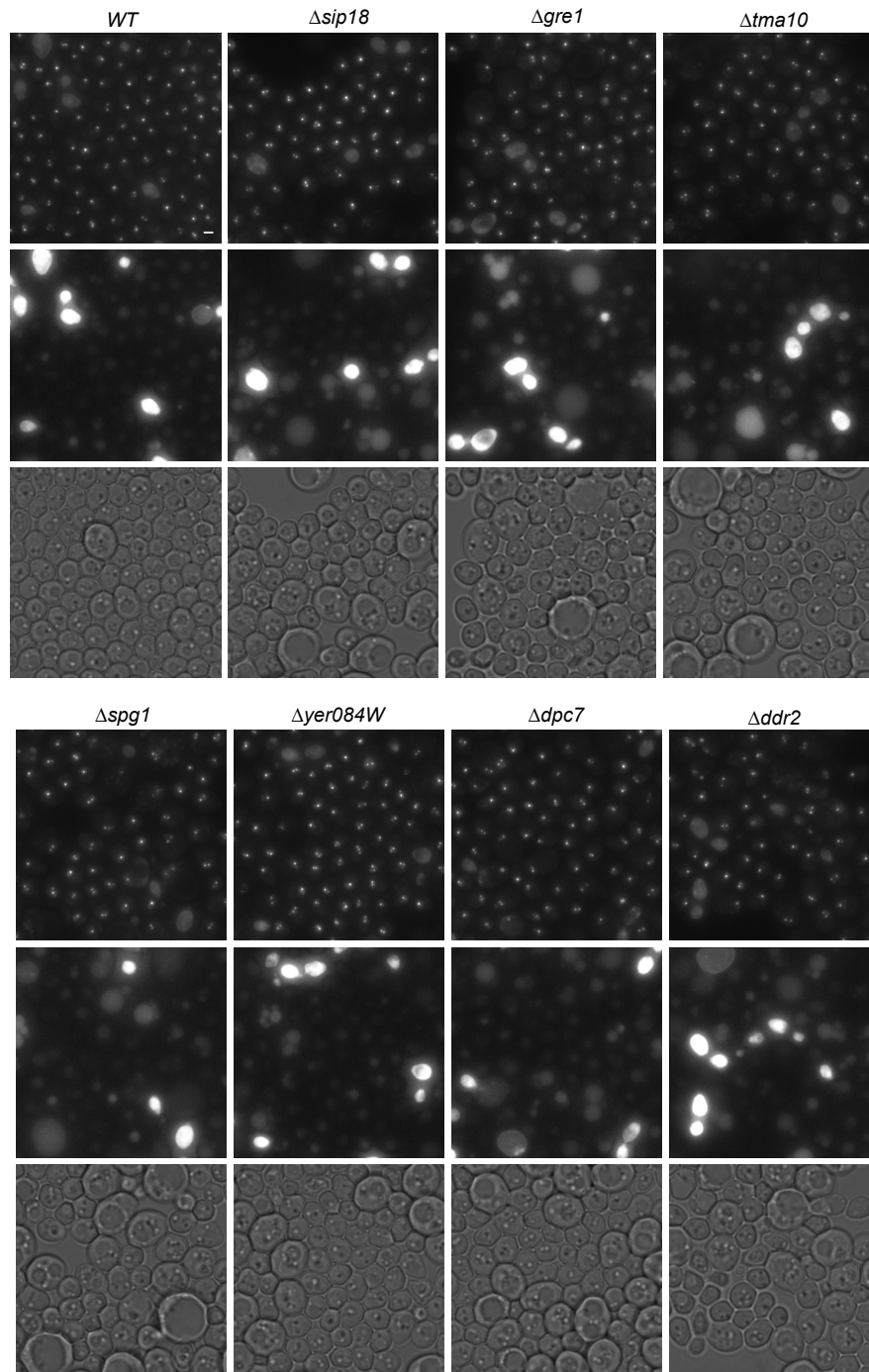
S3K

a) LOG



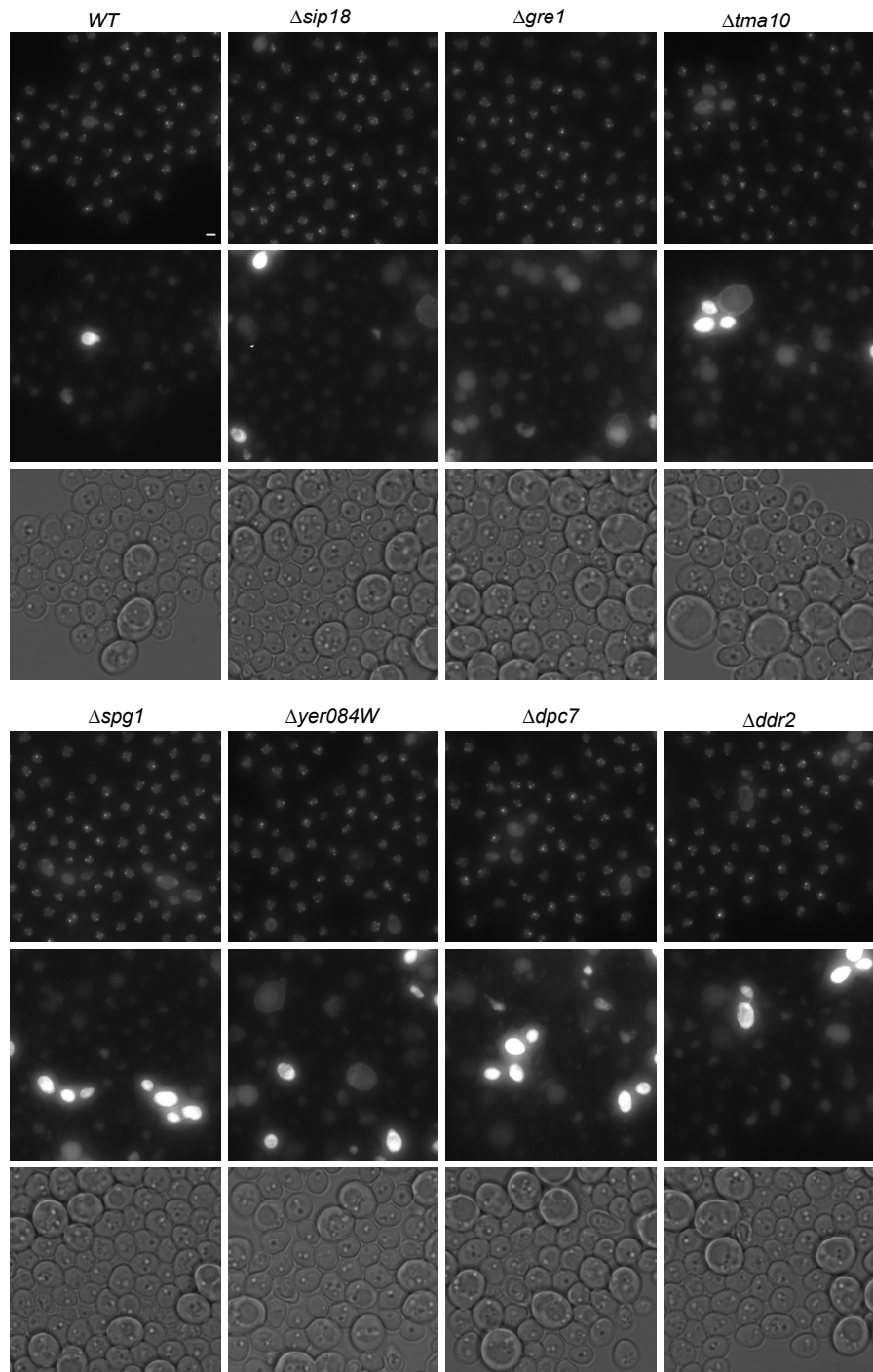
S3K

b) STATIONARY PHASE



S3K

c) 30 MIN RELEASE



Supplemental Figure S3

K. Representative images of Rap1-GFP and Hxt1-mCherry in mutants of the top Q genes (described in Fig 3C), sampled in a) exponentially growing cells (LOG), b) after 6 days of rich medium exhaustion (stationary phase) and c) 30 minutes post-refeeding (release). Brightness for all Rap1-GFP images is set at 1600 maximum and Hxt1-mCherry at 700 maximum. Bar = 1 μ m

Supplemental Figure S4

A

Log

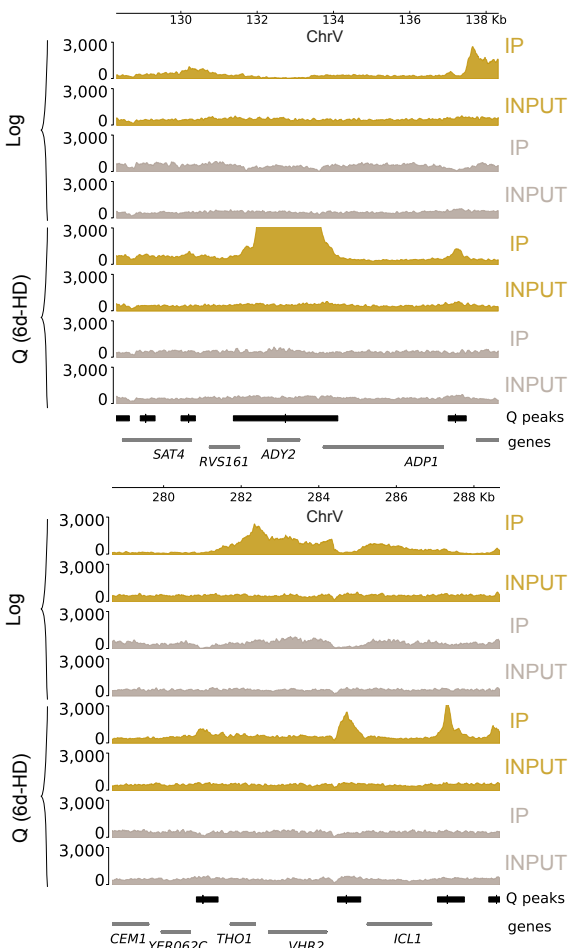
intergene type	no peak	with any peak	total
convergent	843	723	1566
tandem	1792	1052	2844
divergent	1088	405	1493

Q

intergene type	no peak	with any peak	total
convergent	1338	228	1566
tandem	1776	1068	2844
divergent	788	705	1493

B

WT Rpb3-FLAG
WT Rpb3 untagged

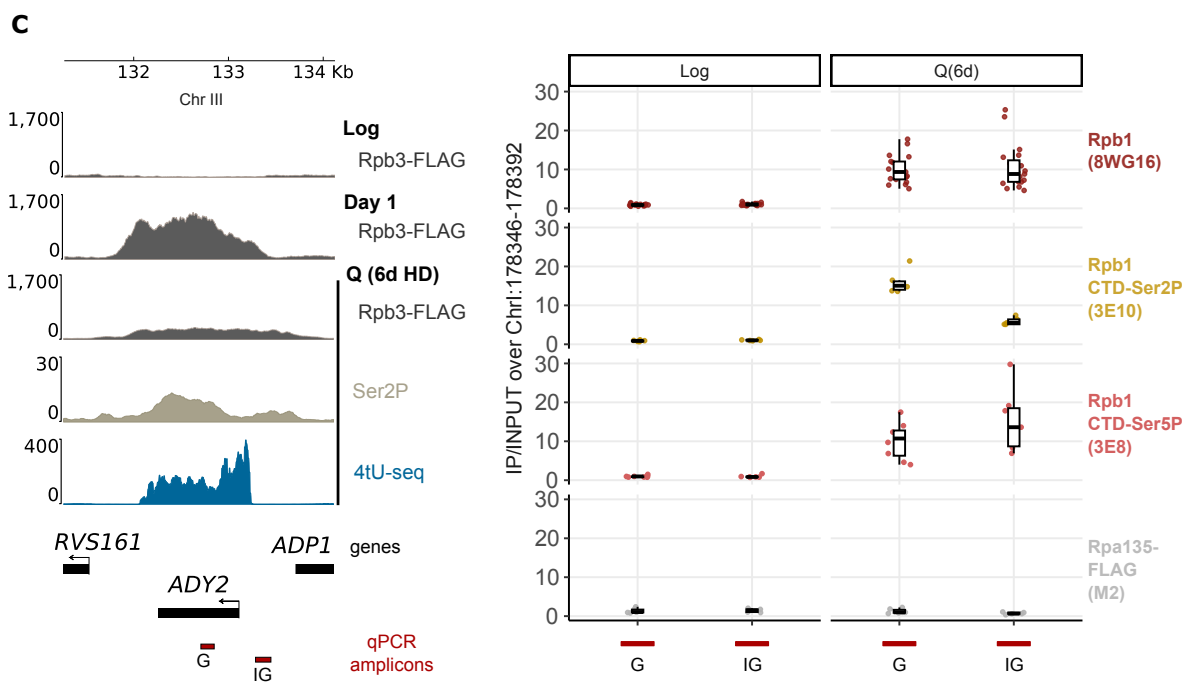


Supplemental Figure S4

A. Number of intergenes by type overlapped or not by an RNAPII peak (methods) in Log cells (*top*) and quiescent (6d-HD) cells (*bottom*).

B. Genomic windows showing coverage tracks of Rpb3-FLAG ChIP-seq samples and controls. Dark yellow: yAT3239 strain, bearing Rpb3-FLAG tag. Grey: yAT1684 strain with Rpb3 WT protein. MACS2

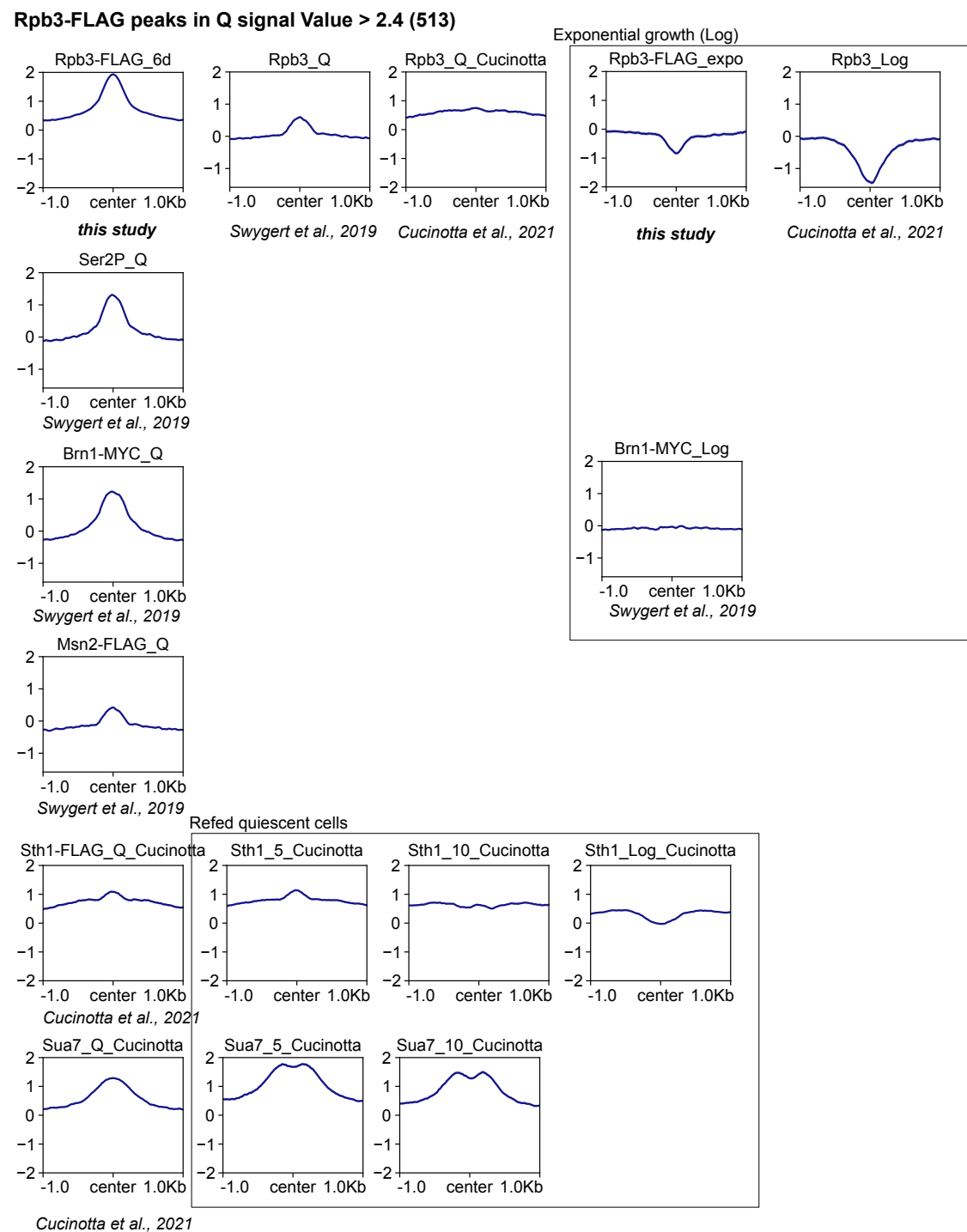
called-peaks are depicted above the annotations as black bars. Summits are shown as vertical lines intersecting the peaks.



Supplemental Figure S4

C. Mapping of RNAPII (Rpb1 C-terminal domain, Rpb1 CTD; Rpb1 CTD Serine 2 phosphorylation, Rpb1 CTD-Ser2P; Rpb1 CTD Serine 5 phosphorylation, Rpb1 CTD Ser5P) and RNAPI (Rpa135-FLAG) epitopes in the coding sequence (G) and in the upstream intergene (IG) of the *ADY2* gene (class I gene). (left) Genome browser view of spike-in calibrated Rpb3-FLAG (this study), Rpb1 CTD Serine 2 phosphorylation (Rpb1 CTD-Ser2P, Swygert et al., 2019) and recently synthesized transcripts (4tU-seq, both strands merged, Cucinotta et al., 2021). (right) ChIP-qPCR IP/INPUT signal normalized to an intergenic region in ChrI (methods). Antibodies used are written in parentheses.

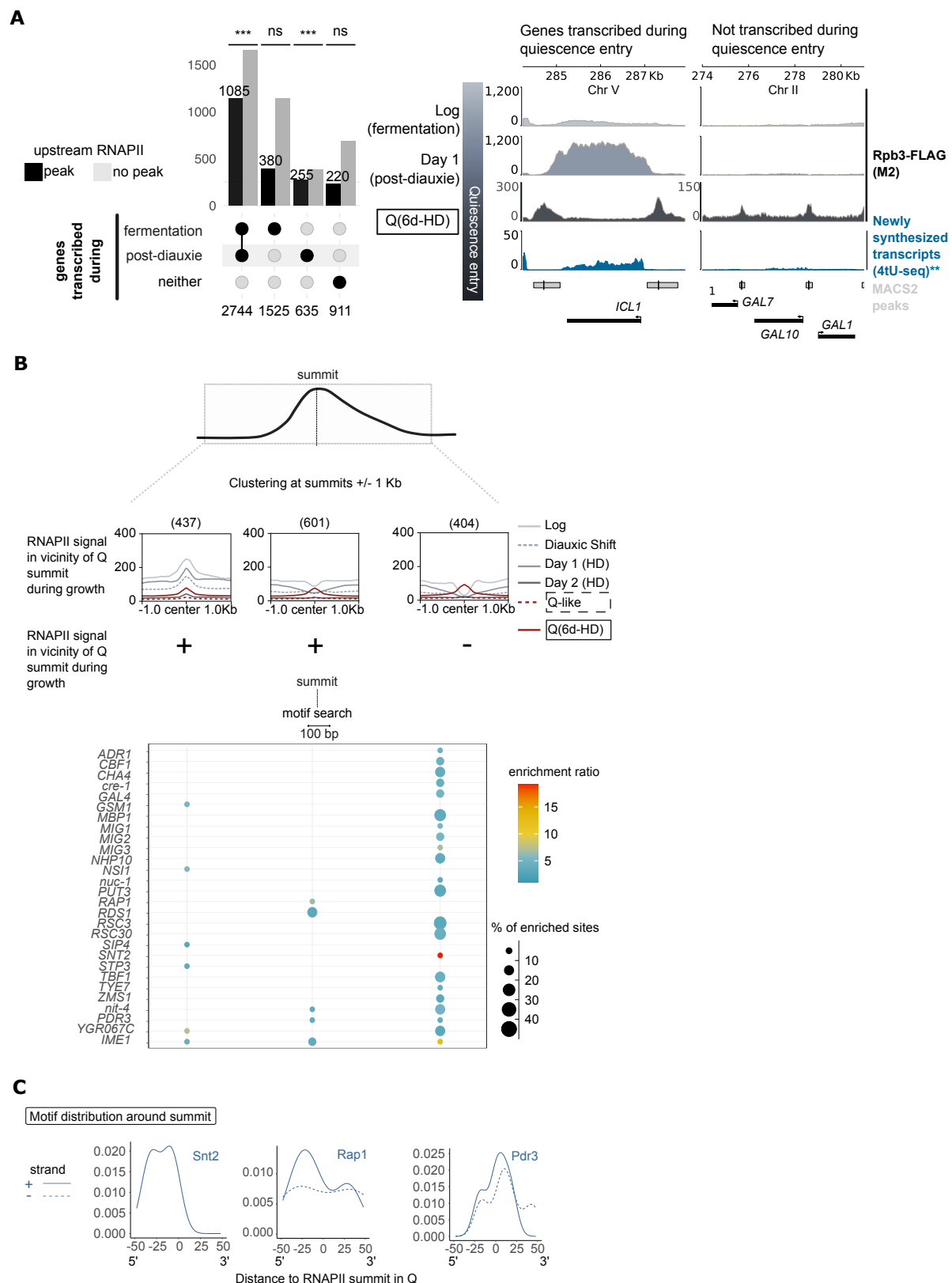
D



Supplemental Figure S4

D. Average profile of published mappings in log phase, quiescent or refed quiescent cells piled-up at summits (center) of RNAPII peaks (MACS2 signal Value > 2.4) falling in promoters, as defined in Fig 4C. Note that Rpb3 ChIP signal from Swygart et al., 2019 is clearly enriched at Rpb3-FLAG peaks, unlike that from Cucinotta et al., 2021, possibly due to variations in ChIP efficiency. However, Rpb3 ChIP from Cucinotta et al., 2021 is much higher in Q than in Log phase at these loci.

Supplemental Figure S5



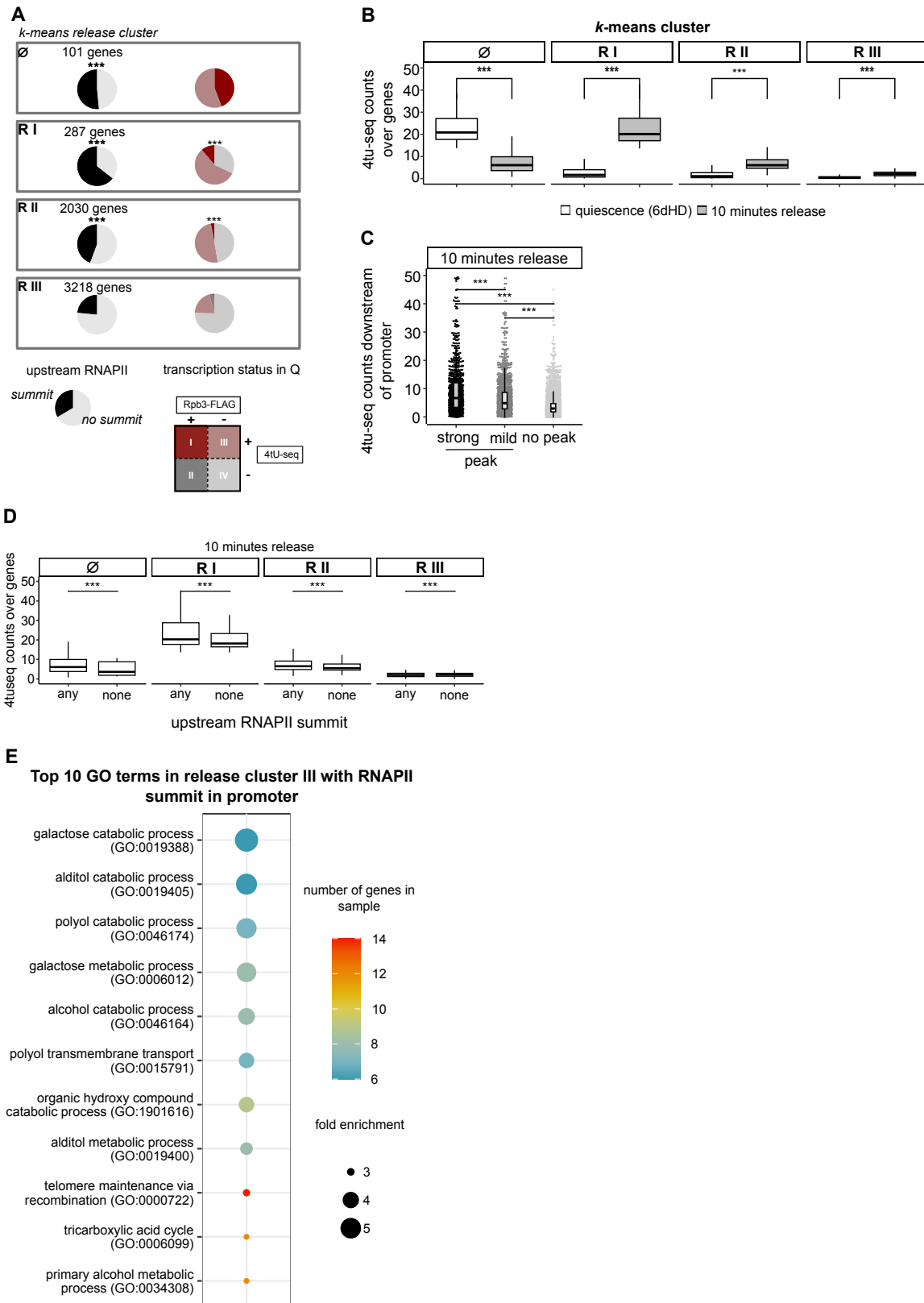
Supplemental Figure S5

A. (left) UpSet plot shows overlap of genes transcribed during fermentation (Log), respiration (post-diauxie, day 1 HD), or neither, based on the average Rpb3-FLAG counts as in Fig 3A. For each intersection, genes bearing RNAPII at the promoter are shown as bar counts in black. (hypergeometric test, transcribed only during post-diauxie, $p\text{-value}=6.02\text{e-}05$; transcribed in both fermentation and respiration, $p\text{-value}=1.31\text{e-}21$) (right) Genome browser view depicting Rpb3-FLAG (this study) and newly synthesized transcripts (Cucinotta et al., 2021) at representative genes transcribed or not during quiescence entry and bearing an upstream RNAPII peak.

B. Transcription factor binding sites (TFBS, JASPAR 2022 fungi database (Castro-Mondragon et al. 2022)) found in the vicinity (100 bp) of RNAPII intergenic summits for each category described in Fig 5C, with a fold enrichment over control > 3 (SEA, MEME suite (Bailey and Grant 2021)).

C. Distribution of binding motifs for the top 3 TFBS relative to the peak's summit (0). Binding sites are oriented such that negative values are sites upstream of the summit.

Supplemental Figure S6



Supplemental Figure S6

A. Proportion of genes in each category of transcription status described in fig. 3A per k-means cluster of recently synthesized transcripts described in fig. 6A. (left) *** indicate significant enrichment in RNAPII summits at promoter, as described in fig. 6A. (right) p-values (hypergeometric test) correspond

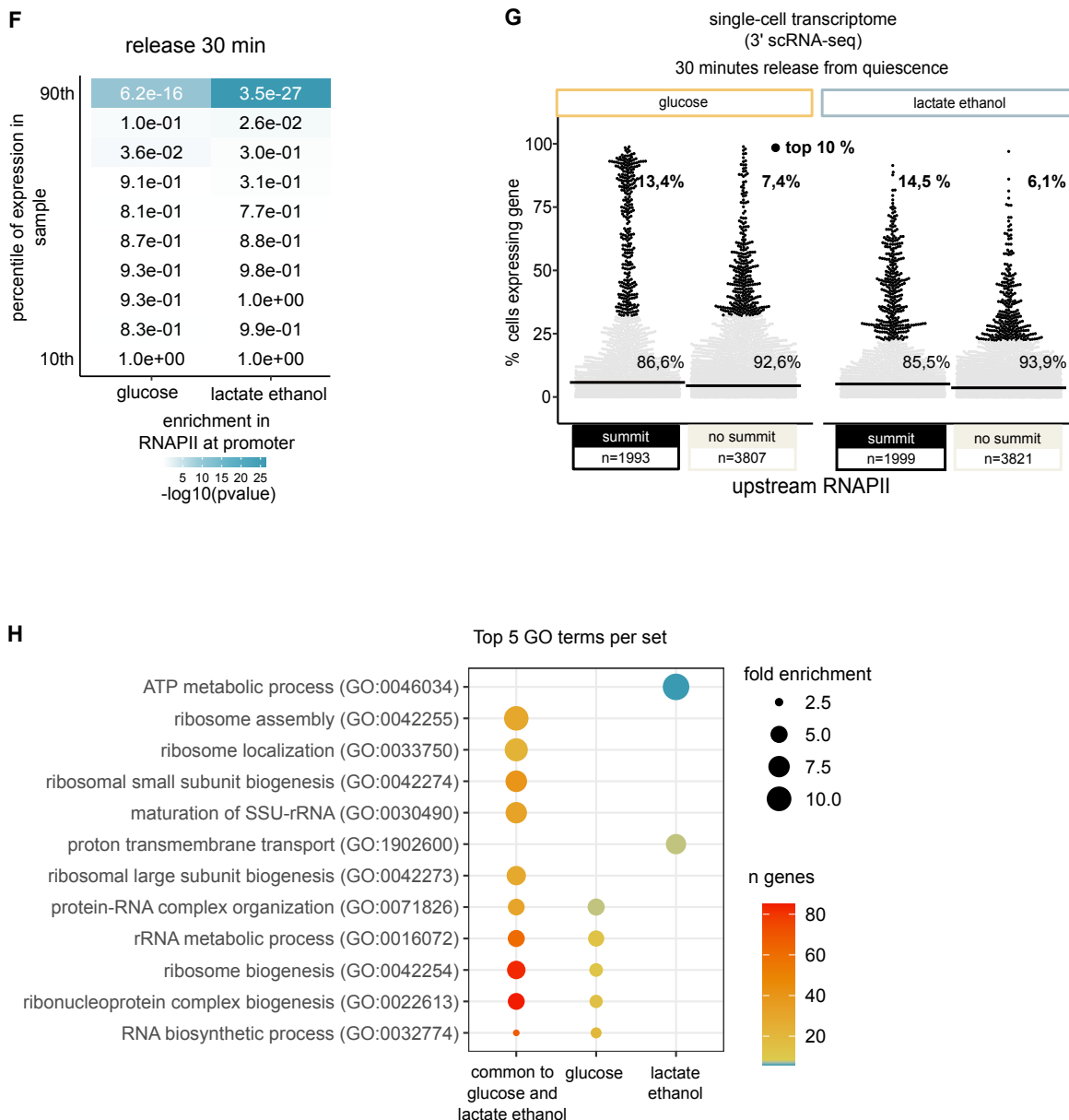
to enrichment in genes with evidence for transcription (class I or III, as defined in fig. 3A; R I, 3.45e-31; R II, 2.45e-82)

B. Recently synthesized transcripts counts (4tu-seq) over genes for each cluster described in fig. 6A, in quiescent samples (6dHD) and refed quiescent samples after 10 minutes.

C. Recently synthesized transcripts counts (4tu-seq) in refed quiescent samples (10 minutes) over genes bearing a strong (signal value > 2.4), mild (signal value =< 2.4) or no RNAPII MACS2 called peak in the promoter

D. Recently synthesized transcripts counts (4tu-seq) in refed quiescent samples (10 minutes) over genes bearing (any) or no (none) RNAPII summit in the promoter for every k-means cluster described in fig. 6A

E. Top 10 Gene Ontology terms significantly enriched (p value > 0.05) for genes in release cluster R III and bearing RNAPII in the promoter.



Supplemental Figure S6

F. p-values for heatmap of RNAPII enrichment at promoter per decile of expression shown in F6B. Enrichment was estimated by a hypergeometric test (p-values shown in S6F).

G. Percentage of cells released in glucose or lactate-ethanol expressing genes with or without an upstream RNAPII summit. The top 10% of the distribution for either sugar is highlighted in black. Shown on top are the percentages that the top 10 and bottom 90% of genes represent for each category (summit or no summit).

H. Top 5 Gene Ontology terms significantly enriched (p value > 0.05) for genes bearing RNAPII in the promoter and found in the top 10% of expression of glucose-released only (54 genes), lactate-ethanol-released (70 genes) quiescent cells, or both (common, 219 genes).

Supplemental Materials and Methods

HD gradient enrichment

For ChIP-seq experiments 4.8×10^9 (400 OD₆₀₀) cells were collected and re-suspended in sterile water to reach 1.2×10^7 cells/mL (1 OD₆₀₀/mL). Cross-linked or live cells (for Q-like, see below) were pelleted at 4000 rpm for 20 minutes, washed and re-suspended in 50 mM Tris pH 7.5, 1× for sorting. Then, cells were loaded over a pre-established salt gradient as follows. A 11.5 mL solution of 150 mM NaCl in Percoll (Sigma) was established in 14 mL ultraclear Beckman Coulter tubes by centrifugation in a SW40Ti swinging-bucket rotor at 19000g for 20 minutes. Then, 133 OD₆₀₀ of crosslinked cells were loaded per gradient and centrifuged at 400g for one hour in swing buckets. The lower fraction, corresponding to highly dense (HD) cells, was collected, and washed twice with TBS 1× pH 7.6. HD-enriched fractions were identically enriched from 6 days stationary phase live cultures for release from quiescence scRNA-seq experiments. For transcription and translation inhibition experiments, a modified version of the protocol, adapted from (Leonov et al. 2017), was performed. Briefly, we used 5 mL ultraclear tubes to establish the gradients at 25000 g in an MLS50 rotor, then loaded 125 OD₆₀₀ of live cells in 50 mM Tris pH 7.5 per gradient and centrifuged at 1000g for 30 minutes.

Imaging and Rap1-GFP foci quantification

Images were acquired on a wide-field microscopy system driven by MetaMorph software (Molecular Devices), based on an inverted microscope (Nikon TE2000) equipped with a 100×/1.4NA immersion objective. Images were captured using a C-mos camera (ORCA-flash C11440, Hamamatsu, Japan), and a Spectra X light engine lamp (Lumencor, Inc, Beaverton, OR, USA). Images shown are maximum intensity z-

projections of z-stacks acquired with a 200 nm step. For any given experiment, all images are taken with the same acquisition parameters.

Quantification of Rap1-GFP foci was performed using an in-house algorithm, NuFoQ, adapted from Guidi et al. 2015. Briefly, z-stack images were deconvolved with Huygens Remote Manager 3.9 ((Montpellier RIO Imaging (CNRS) 2023)). Based on deconvolved images, NuFoQ (<https://github.com/mgPICT/NuFoQ>) fully segments spots in 3D and extracts their intensities as total integrated pixel values from raw images. Rap1-GFP total nuclear signal is taken as nuclear staining. For Fig 1B, 2A and Supplemental Fig 1A, cluster (focus) intensities are calculated relative to nuclear staining. For each timepoint, the average intensity of clusters is assessed (i_{cluster}). A hypercluster is defined as having an intensity $i_{\text{cluster}} \geq 4 \times \text{median}(i_{\text{clusters}})_{\text{Log cells}}$ (Fig 1), or $i_{\text{cluster}} \geq 4 \times \text{median}(i_{\text{clusters}})_{\text{120 min release}}$ (Fig 2). Proportions in pie charts represent nuclei with at least one hypercluster.

Sample harvesting for chromatin immunoprecipitation

To recover only the highly dense population as cells progress into stationary phase in the nutrient exhaustion kinetics, all samples after diauxic shift (24h, 48h, Q6d) were crosslinked, then purified by gradient sorting. 4.8×10^9 (400 OD₆₀₀) cells were collected and re-suspended in sterile water to reach 1.2×10^7 cells/mL (1 OD₆₀₀/mL) and immediately cross-linked with 1% paraformaldehyde (32% stock solution, Sigma) for 15 minutes, shaking, at room temperature, then quenched for 5 minutes with 2.5 M glycine (125 mM final). Then, crosslinked cells were pelleted at 4000 rpm for 20 minutes, washed and re-suspended in 50 mM Tris pH 7.5, 1×, before sorting on a density gradient (see above). The lower fraction, corresponding to highly dense (HD) cells, was collected, and washed twice with TBS 1× pH 7.6. 100OD₆₀₀ were pelleted

and flash-frozen in liquid nitrogen for storage at -80 °C before ChIP. To harvest Q-like cells for ChIP (quiescence by abrupt starvation), 400 OD₆₀₀ of live cells were gradient-sorted after 24h of growth in YPD following the protocol described above. Then, 100 OD₆₀₀ of highly dense cells were washed and re-suspended in H₂O for 24h, before cross-linking and pelleting as above.

S. cerevisiae culture on exponential phase or at the DS, as well as *S. pombe* samples used as spike-in for ChIP-seq were harvested in the same manner for ChIP: crosslinked, then flash-frozen as described above.

ChIP-seq

Two biological replicates were processed independently for chromatin immunoprecipitation, and all libraries for sequencing were prepared simultaneously. Unless indicated, all the following steps were carried out at 4°C. For every 20 OD₆₀₀ of cells, 40 µL of protein G magnetic beads (New England Biolabs) were washed with wash and bind buffer(0.1M NaP, 0.01% Tween 20 pH 8.2), 7.5% BSA was added and incubated on a spinning wheel at 4°C for 3h. 4 µL of FLAG antibody (Sigma-Aldrich, M8823) was added to every 4 µL of protein G magnetic beads, which were then incubated on a spinning wheel at 4°C for 4h.

Pellets were thawed and re-suspended in 500 µL of IP buffer (20% SDS, 20% Triton X- 100, 0,5M EDTA pH 8.0, 1M Tris pH 8.0, 5M NaCl, 7,5 % BSA, 10 mg/ml tRNA) with 2,5µL of Protease Inhibitor (Sigma-Aldrich P1816) and 2 OD_{600 nm} equivalent of calibration cells (*S. pombe*) for every 100 OD_{600 nm} of experimental cells. Using a FastPrep instrument (MP Biomedicals), exponential phase samples were mechanically lysed with 500 µm zirconium/silica beads (Biospec Products) by three cycles of 30 sec, intensity (6msec⁻¹). All other samples were lysed with 710-1180 µm

glass beads (SIGMA, G1142) by five cycles of 30 sec, intensity (6msec⁻¹). Each bead beating cycle was followed by 5 min incubation on ice. Chromatin corresponding to 100 OD_{600nm} was fragmented in 15 mL Bioruptor tubes (C30010017) to a minimum 200 bp and average size of 450 bp by sonication using Bioruptor Pico (Diagenode) for 30 min at high power with 30 sec on/30 sec off. Lysate was centrifuged 10 min at 4,500 rpm and 10 μ L were saved as whole cell lysates (INPUT DNA). Antibody and protein G beads were recovered using a magnetic beads purification magnet (Invitrogen) and re-suspended in cleared lysate for incubation overnight on a spinning wheel. Magnetic beads were washed sequentially with lysis buffer, twice with RIPA buffer (0.1% SDS, 10 mM Tris at pH 7.6, 1 mM EDTA at pH 8, 0.1% sodium deoxycholate, and 1 % Triton X- 100), twice with RIPA buffer supplemented with 300 mM NaCl, twice in LiCl buffer (250 mM LiCl, 0.5% NP-40, 0.5% sodium deoxycholate), with TE 0.2% Triton X-100 and with TE. Input was diluted 10 \times with elution buffer (50 mM Tris, 10 mM EDTA at pH 8, 1% SDS) and beads were resuspended in 200 μ L elution buffer, then incubated, shaking at 800 rpm, for 20 minutes at 65°C. Proteins were digested with Proteinase K at 0,1 mg/mL. Crosslinking reversal was performed by heating samples overnight at 65°C. Samples were treated with RNase A for 1h at 37°C, and the remaining DNA was purified on QIAquick PCR purification columns.

DNA quantification and size distribution profiles were performed with Qubit®dsDNA HS Assay Kit and TapeStation HS (Agilent) respectively. Libraries were prepared with TruSeq®ChIP Illumina kits. All libraries were amplified with 12 PCR cycles.

ChIP-qPCR experiments

Samples for ChIP-qPCR experiments were harvested as described above for ChIP-seq on Rpb3-FLAG. Whenever immunoprecipitation was performed on Ser2-(3E10 clone, MercK-Millipore 04-1571, 5 μ L for 20 OD_{600nm}) or Ser5-(3E8 clone, Active Motif

61085, 5 µl for 20 OD_{600nm}) phosphorylations of the CTD, the Rpb1 CTD (clone 8WG16, Biolegend, 4 µl for 20 OD_{600nm}) was targeted in parallel, with the same batch of crosslinked cells. Quantitative PCR (qPCR) measurements were performed on the QuantStudio 5 Real-Time PCR System (Applied Biosystems, Waltham, MA, USA). Target amplicons (defined by the primers listed in table Supplemental Table S3) were amplified using the SYBR Green PCR Master Mix (Applied Biosystems, Waltham, MA, USA) on a dilution of immunoprecipitated DNA (IP) at 1/40 and 1/80 for the input DNA. PCR reactions were conducted using the following program: an initial denaturation at 95°C for 10 min followed by 40 cycles (95°C for 15 s and 60°C for 30 s). Each real-time PCR reaction was performed at least in triplicate. The number of replicates shown on ChIP-qPCR figures (N) corresponds to biological replicates, for which technical qPCR replicates are averaged. As positive control for all IPs, all qPCR measurements routinely included the primers targeting RPL3 gene body amplicons (listed in table Supplemental Table S3). The signal from every targeted amplicon was normalized to a control locus in an intergenic region (Chr1:178346- 178392, target N411 in Supplemental Table S3) that does not show significant variations throughout the quiescence induction kinetics (as assessed by visual examination of z-score normalized signals).

ChIP-seq data processing

Rpb3-FLAG ChIP-seq libraries were sequenced (single-end 50 (HiSeq-Rapid Run)) at the Institut Curie NGS platform. WT samples (yAT1684 and yAT3239) were sequenced together. WT IP samples for Log and Q (6dHD) were re-sequenced together with *sir3Δ* samples in a different run. Thus, they were treated separately for analysis. For mapping, reads were competitively aligned to a hybrid *S. pombe* (ASM294v2.28) and *S. cerevisiae* genome (SGD Project 2015), with Bowtie 2 (bowtie2-align-s -p 8 ,

(Langmead and Salzberg 2012)). To visualize sub-telomeric genes, filtering was performed to allow up to three mismatches (grep -E “(^@|XM:i:[0-3])”).

To calibrate the ChIP signal, an occupancy ratio (OR) was calculated based on the number of uniquely mapped reads to either genome (experimental: *S.cerevisiae*, spike-in: *S. pombe*), present in IP and INPUT samples of the Rpb3-FLAG tagged (yAT3239) and Rpb3 untagged (yAT1684) strains, as described in (Hu et al. 2015). OR was used as a scaling factor to generate coverage tracks from IP samples (shown in all genome browser snapshots, and average profile plots, except when compared to other mappings, in Fig 4D and Supplemental Fig S4C, see below), using deepTools (3.5.0) (Ramírez et al. 2016) BamCoverage with RPKM normalization. The coverage for all IP and INPUT samples is depicted in Supplemental Figure S4B.

Peak calling, counts and thresholding

Peak calling was performed using both biological replicates with MACS2 (Zhang et al. 2008), using as treatment the IP from tagged Rpb3-FLAG samples (yAT3239) and as controls the IP from untagged Rpb3 (yAT1684) samples (MACS2 callpeak -t "\$IP_1" "\$IP_2" -c "\$ctrl_1" "\$ctrl_2" -g 1.2e+7 -f BAM --verbose 3 -q 0.001 -m 10 30 --nomodel --extsize 200 --keep-dup all). Strong peaks (Fig 4D; Supplemental Fig S6C) were defined as having a signalValue (MACS2) > 2.4 after visual inspection of the narrowPeak file in IGV. To determine the fraction of intergenes overlapped by a peak (Supplemental Figure S4A, Supplemental Table S5), or the promoters overlapped by peaks (S6C), the intersect function in BEDTools (Quinlan and Hall 2010) was used. All counts on Rpb3-FLAG of the quiescence induction kinetics were generated with deepTools(3.5.0) (Ramírez et al. 2016) multiBigWigSummary (Fig 1B; Supplemental Fig S3A,B,D) on calibrated coverage files and thus take the OR scaling factor into account. Except for FigS3A the average of two replicates, calculated using wiggletools

(Zerbino 2020), is shown. For Fig 1C, deepTools multiBigWigSummary was used to obtain counts normalized to gene size, from mapped IP samples. To determine the threshold for average Rpb3-FLAG counts over gene bodies, the average counts under significantly called peaks (50) were used as reference. For 4tU-seq counts, and because the aim was to detect any transcription, the threshold was set at 1 average count over gene body, since it reflected CDS with minimal, but homogeneous coverage, as visually inspected on Integrative Genome browser (IGV, (Thorvaldsdottir et al. 2013)). To determine the fraction of strong summits with recently synthesized transcripts, multiBigWigSummary was used as described above, using regions defined as summit +/- 50 bp as input. Same threshold as for gene bodies was applied (1 average count over the region).

Integration with published datasets

To compare Rpb3-FLAG mappings to published (processed) ChIP-seq or ChIP-array datasets, zscores were calculated using wiggletools (Zerbino 2020) and awk. For Rpb3-FLAG, zscores were calculated from $\log_2(\text{IP}_{\text{WT}}/\text{INPUT}_{\text{WT}}) - \log_2(\text{IP}_{\text{untagged}}/\text{INPUT}_{\text{untagged}})$. For all published mappings in figures 4D and S4C, z-scores were calculated directly from published processed files. 500 random locations in promoter-bearing intergenes were sampled as controls. To plot the density distribution in Fig 5A, TSS annotated by CRAC-seq in cycling cells (kindly shared by Domenico Libri) were used. 4tU-seq reads from (Cucinotta et al., 2021) trimmed (trim_galore, (Krueger et al. 2023)) and re-mapped to the R64_2-1 assembly with hisat 2.2.1 (HISAT2 –max-intronlen 5000, (Kim et al. 2019)) then sorted (samtools view -F 256,2048, (Danecek et al. 2021)). Coverage files were generated with deepTools (3.5.0) BamCoverage with CPM normalization. For Fig 5A, sequences corresponding to annotated UAS, curated in (Schofield and Hahn 2023) were retrieved using BLAST+ (Camacho et al. 2009). Only those 4133 uniquely mapping with less than three mismatches were used. The number of summits within these annotated UAS was retrieved using BEDTools intersect (Quinlan and Hall 2010).

Motif and Gene Ontology enrichment analyses

Motif search was performed as follows. Sequences spanning 50 base pairs around the indicated peaks' summits were generated with BEDTools slop and getfasta to be used as samples. For controls, locations at 250 base pairs upstream of TSS in promoter-bearing intergenes without any RNAPII peak overlap were treated the same way. Samples and controls were used as input in SEA from the MEME suite (Bailey and Grant 2021), using the JASPAR 2022 fungi database (Castro-Mondragon et al. 2022) and requiring an E-value ≥ 1 . Factors shown in Fig 5C are filtered for an

enrichment ratio > 3. Gene Ontology statistical overrepresentation test analyses (Fisher test, FDR correction) were performed using PantherGO (Thomas et al. 2022; Mi et al. 2019). Results were sorted and filtered in R to retrieve the top 5 GO terms in Supplemental Fig S3G, the top 10 GO terms with hierarchy = $<$ 5 in Supplemental Fig S6E, or the top 5 GO terms with hierarchy = $<$ 2 in Supplemental Fig S6H. Results were processed using tidyverse packages (Wickham et al. 2019) and plotted using ggplot2 (Wickham 2016).

Clustering

k-means clustering was performed with the computeMatrix and plotHeatmap functions in deepTools (Ramírez et al. 2016). For Fig 5D, clustering was performed using all samples in the kinetics on the piled-up signal centered at Q summits, extended 1kb up- and downstream of the summit, using the refPoint mode. For Fig 6A, clustering was performed using Q and 10 min release samples on scaled coding sequences binned at 10 bp, using the scaleRegions mode.

Figure preparation

Heatmaps and average profile plots were generated with plotHeatmap and plotProfile from deepTools(3.5.0)(Ramírez et al. 2016). All counts matrices computed with computeMatrix or multiBigWigSummary were masked for all rDNA loci. Genome Browser figures were generated with pygenometracks(3.7) (Lopez-Delisle et al., 2021). All other plots and analyses were generated using R Statistical Software (R version 4.3.3 2024-02-29, (R Core Team 2021)), with the packages listed in Supplemental Table S6. Figures were annotated and assembled using inkscape (Inkscape Project 2022).

scRNA-seq experiments

Initially, the cell quantity was estimated from the concentration of the cell suspension in OD_{600nm}/mL. After fixation, cell concentration was determined by flow cytometry. At least double the required number of cells were harvested to ensure sufficient volume for ongoing measurements. The cell suspension volume calculator table was referenced for adjustments. For instance, to harvest 10,000 cells, a 0.2 OD_{600nm} equivalent (e.g., 200 μ L of cell suspension at 1 OD/mL) of gradient-enriched quiescent cells (6d-HD, see above), or quiescent cells refed for 30 minutes, was collected in a 2 mL Eppendorf tube, centrifuged for 4 minutes at 2500 rpm, and the supernatant was removed. Chilled 80% methanol (1.6 mL) was added dropwise to the pellet, incubated at -20°C for 30 minutes, and then stored at -20°C or processed further. For rehydration and counting, methanol-fixed cells were equilibrated to 4°C, centrifuged for 4 minutes at 2500 rpm, and the supernatant was removed, leaving about 1 μ L to evaporate. 1 mL of wash-resuspension buffer (1 mM DTT, 200 U/mL RNase inhibitor (RiboSafe RNase Inhibitor BIO-65028, Meridian Bioscience), 0.04% BSA, diluted to volume with PBS) was added to the pellet and mixed. The sample was split into two portions: S1 was stored at 4°C, and S2 was used to assess cell concentration using the Attune NxT Flow Cytometer. The cell suspension volume calculator table was used to determine the dilution needed to reach 700-1200 cells/ μ L. Dilutions were made from S1 before proceeding with step 1.2b of the 10 \times single-cell protocol.

scRNA-seq data processing

Mapping and count matrices

Sample demultiplexing, barcode processing and single cell 3' counting were performed using 10x Genomics Cell Ranger v7.1.0 (Zheng et al. 2017). For Fig 3 and

6, only those protein-coding annotations considered for ChIP-seq analyses found in both datasets were kept.

Filtering

Count matrices were processed using Jupyter Notebooks (v6.5.4) and Python (v3.8.11). For the filtering and normalization, the Python packages: SCANPY (v1.9.8) (Wolf et al. 2018), Scrublet (Wolock et al. 2019) and Scran (v0.1) (Fortmann 2024) were used. For both the quiescent and 30 min release samples, cells were filtered out if they had fewer than 100 detected genes and fewer than 150 UMI counts. For the quiescent sample, outlier cells with more than 1000 UMI counts were not included, while for 30 min release sample, outlier cells with more than 12500 UMI counts were removed. This filtering resulted in 30,270 and 15536 cells, for the quiescent and 30 min release samples respectively. Doublet detection and filtering was carried out using Scrublet (Wolock et al. 2019), using an expected doublet rate of 2%, iteratively running the filter until the estimated doublet rate was below 10%. This resulted in 5618 cells and 8092 cells for the quiescent sample and 30 min release samples respectively. Genes not detected in the populations were filtered out.

Normalization, dimensionality reduction and visualization

For the quiescent sample, normalization was performed using Scran to account for variable UMI counts across cells. Sum factors were calculated using `scrPY.compute_sum_factors` with parameters `parallelize=True`, `algorithm='CVXPY'`, and `max_size=3000`. The size factors ranged from 0.061 to 5.782, and counts were normalized by dividing by these size factors. Then, the size-factor adjusted data was `log1p`-transformed using Scanpy.

Highly variable genes were identified using Scanpy, `n_top_genes=5500`. Principal Component Analysis (PCA) was initially performed with 50 components

(n_comps=50), followed by a second PCA with eight components based on the shoulder of the variance ratio distribution. Neighbors were computed using the PCA results, and UMAP coordinates were generated. The expression of Class I genes was calculated as proportion of the cellular transcriptome. Data was denormalized and reconfigured with the following formula:

$$\% \text{ of transcriptome (Class I genes)} = \frac{\text{size factor} \times \sum(e^{\text{Class I UMI counts} - 1})}{\text{Total UMI counts cell}} \times 100$$

UMAP plots were generated to visualize the spatial distribution of Class I gene expression using Matplotlib (The Matplotlib Development Team 2024) and Scanpy's plotting functions.

RNA-seq data processing

Reads were trimmed (trim_galore, (Krueger et al. 2023)) and mapped to the R64_2-1 assembly with hisat 2.2.1 (HISAT2 –max-intronlen 5000, (Kim et al. 2019)) then sorted (samtools view -F 256,2048, (Danecek et al. 2021)). Coverage files were generated with deepTools (3.5.0) BamCoverage with CPM normalization and counts over coding genes were performed with multiBigWigSummary, then visualized with ggplot2 in R.

Supplemental References

Bailey TL, Grant CE. 2021. SEA: Simple Enrichment Analysis of motifs. 2021.08.23.457422. <https://www.biorxiv.org/content/10.1101/2021.08.23.457422v1> (Accessed July 29, 2024).

Camacho C, Coulouris G, Avagyan V, Ma N, Papadopoulos J, Bealer K, Madden TL. 2009. BLAST+: architecture and applications. *BMC Bioinformatics* **10**: 421.

Castro-Mondragon JA, Riudavets-Puig R, Rauluseviciute I, Berhanu Lemma R, Turchi L, Blanc-Mathieu R, Lucas J, Boddie P, Khan A, Manosalva Pérez N, et al. 2022.

JASPAR 2022: the 9th release of the open-access database of transcription factor binding profiles. *Nucleic Acids Res* **50**: D165–D173.

Danecek P, Bonfield JK, Liddle J, Marshall J, Ohan V, Pollard MO, Whitwham A, Keane T, McCarthy SA, Davies RM, et al. 2021. Twelve years of SAMtools and BCFtools. *GigaScience* **10**: giab008.

Fortmann S. 2024. sfortma2/scranPY. <https://github.com/sfortma2/scranPY> (Accessed July 31, 2024).

Guidi M, Ruault M, Marbouth M, Loïodice I, Cournac A, Billaudeau C, Hocher A, Mozziconacci J, Koszul R, Taddei A. 2015. Spatial reorganization of telomeres in long-lived quiescent cells. *Genome Biol* **16**: 206.

Hu B, Petela N, Kurze A, Chan K-L, Chapard C, Nasmyth K. 2015. Biological chromodynamics: a general method for measuring protein occupancy across the genome by calibrating ChIP-seq. *Nucleic Acids Res* **43**: e132.

Inkscape Project. 2022. Inkscape. <https://inkscape.org>.

Kim D, Paggi JM, Park C, Bennett C, Salzberg SL. 2019. Graph-based genome alignment and genotyping with HISAT2 and HISAT-genotype. *Nat Biotechnol* **37**: 907–915.

Krueger F, James F, Ewels P, Afyounian E, Weinstein M, Schuster-Boeckler B, Hulselmans G, sclamons. 2023. FelixKrueger/TrimGalore: v0.6.10 - add default decompression path. <https://zenodo.org/records/7598955> (Accessed July 31, 2024).

Langmead B, Salzberg SL. 2012. Fast gapped-read alignment with Bowtie 2. *Nat Methods* **9**: 357–359.

Leonov A, Feldman R, Piano A, Arlia-Ciommo A, Lutchman V, Ahmadi M, Elsaser S, Fakim H, Heshmati-Moghaddam M, Hussain A, et al. 2017. Caloric restriction extends yeast chronological lifespan via a mechanism linking cellular aging to cell cycle regulation, maintenance of a quiescent state, entry into a non-quiescent state and survival in the non-quiescent state. *Oncotarget* **8**. <http://www.oncotarget.com/fulltext/20614> (Accessed October 1, 2019).

Mi H, Muruganujan A, Huang X, Ebert D, Mills C, Guo X, Thomas PD. 2019. Protocol Update for large-scale genome and gene function analysis with the PANTHER classification system (v.14.0). *Nat Protoc* **14**: 703–721.

Montpellier RIO Imaging (CNRS). 2023. Huygens Remote Manager. <https://github.com/aarpon/hrm>.

Quinlan AR, Hall IM. 2010. BEDTools: a flexible suite of utilities for comparing genomic features. *Bioinformatics* **26**: 841–842.

R Core Team. 2021. R: A language and environment for statistical ## computing. <https://www.R-project.org/>.

Ramírez F, Ryan DP, Grüning B, Bhardwaj V, Kilpert F, Richter AS, Heyne S, Dündar F, Manke T. 2016. deepTools2: a next generation web server for deep-sequencing data analysis. *Nucleic Acids Res* **44**: W160-165.

Schofield JA, Hahn S. 2023. Broad compatibility between yeast UAS elements and core promoters and identification of promoter elements that determine cofactor specificity. *Cell Rep* **42**: 112387.

SGD Project. 2015. S288C_reference_genome_R64-2-1_20150113.tgz. http://sgd-archive.yeastgenome.org/sequence/S288C_reference/genome_releases/S288C_reference_genome_R64-2-1_20150113.tgz (Accessed June 30, 2019).

The Matplotlib Development Team. 2024. Matplotlib: Visualization with Python. <https://zenodo.org/records/12652732> (Accessed July 31, 2024).

Thomas PD, Ebert D, Muruganujan A, Mushayahama T, Albou L, Mi H. 2022. PANTHER : Making genome-scale phylogenetics accessible to all. *Protein Sci* **31**: 8–22.

Thorvaldsdottir H, Robinson JT, Mesirov JP. 2013. Integrative Genomics Viewer (IGV): high-performance genomics data visualization and exploration. *Brief Bioinform* **14**: 178–192.

Wickham H. 2016. ggplot2: Elegant Graphics for Data Analysis. <https://ggplot2.tidyverse.org>.

Wickham H, Averick M, Bryan J, Chang W, McGowan L, François R, Grolemund G, Hayes A, Henry L, Hester J, et al. 2019. Welcome to the Tidyverse. *J Open Source Softw* **4**: 1686.

Wolf FA, Angerer P, Theis FJ. 2018. SCANPY: large-scale single-cell gene expression data analysis. *Genome Biol* **19**: 15.

Wolock SL, Lopez R, Klein AM. 2019. Scrublet: Computational Identification of Cell Doublets in Single-Cell Transcriptomic Data. *Cell Syst* **8**: 281-291.e9.

Zerbino D. 2020. Wiggletools. <https://github.com/Ensembl/WiggleTools>.

Zhang Y, Liu T, Meyer CA, Eeckhoute J, Johnson DS, Bernstein BE, Nusbaum C, Myers RM, Brown M, Li W, et al. 2008. Model-based analysis of ChIP-Seq (MACS). *Genome Biol* **9**: R137.

Zheng GXY, Terry JM, Belgrader P, Ryvkin P, Bent ZW, Wilson R, Ziraldo SB, Wheeler TD, McDermott GP, Zhu J, et al. 2017. Massively parallel digital transcriptional profiling of single cells. *Nat Commun* **8**: 14049.